Quantum-limited position measurements of a dark matter-wave soliton

Antonio Negretti[1],* Carsten Henkel[2], and Klaus Mølmer[1]
1. Lundbeck Foundation Theoretical Center for Quantum System Research, Department of Physics and Astronomy, University of Aarhus, DK-8000 Aarhus C, Denmark
2. Institut für Physik, Universität Potsdam, Am Neuen Palais 10, D-14476 Potsdam, Germany
(Dated: 27 March 2008)

We show that the position of a dark matter-wave soliton can be determined with a precision that scales with the atomic density as $n^{-3/4}$. This surpasses the standard shot-noise detection limit for independent particles, without use of squeezing and entanglement, and it suggests that interactions among particles may present new advantages in high-precision metrology. We also take into account quantum density fluctuations due to phonon and Goldstone modes and we show that they, somewhat unexpectedly, actually improve the resolution. This happens because the fluctuations depend on the soliton position and make a larger amount of information available.

PACS numbers: 03.75.Nt; 06.20.Dk; 37.25.+k

I. INTRODUCTION

Degenerate quantum gases of atoms and molecules can be trapped in space and their interactions can be controlled by laser and magnetic fields. The spatial quantum state in these gases can be probed in ways unparalleled in other many-body systems. A number of experiments have thus been devoted to exploring their coherence properties by the observation of interference patterns [1] and topological excitations such as solitons and vortices [2, 3, 4]. For application of ultra-cold gases in high-precision metrology, it is a central question how to extract the maximum information from the accessible measurements. We address the case of spatial density measurements on a Bose-Einstein condensate (BEC) with a dark soliton dip, which is a minimum in the atomic density profile. Dark solitons have been produced by slowing down a light pulse using electromagnetically induced transparency (EIT) [4], and the precision probing of the position of such solitons may be used to measure detailed properties of EIT.

It has also been proposed, with a similar setting as in Ref. [5], to use a time-dependent atomic trap guide as a matter-wave interferometer where, after splitting and recombining of a BEC, an oscillating dark soliton is formed [6]. A high-precision determination of the soliton position is crucial here since the amplitude of the soliton oscillation depends on the interferometric phase. The signal-to-noise ratio is in many interferometric experiments given by the standard shot noise, leading to a phase resolution that scales with $1/\sqrt{N}$, where N is the number of detection events. The normal interference fringes in a matter-wave interferometer are located in accordance with the interferometer phase and yield the same dependence on the number density. Special quantum features such as entanglement and squeezing imply that this resolution limit is not a fundamental one [7]. In principle, the Heisenberg uncertainty relation provides the optimum sensitivity with a scaling as $1/N$ [8], and for particular entangled states the interferometric phase error scales as $1/N^{3/4}$[9]. Our work will show that the position of a dark soliton can be determined with a precision scaling with the same power law. This result, however, does not rely on squeezing or entanglement. It can be qualitatively understood from counting shot noise, the slope of the mean density versus position, and the $1/\sqrt{n}$ dependence of the soliton width on atomic density due to interactions. Our analysis determines the Fisher information available in the spatial recording of the atomic density and the resulting Crámer-Rao lower bound (CRB) [10] on the determination of the position of the soliton dip.

II. SPATIAL IMAGE OF A DARK SOLITON

The experimental situation we have in mind is sketched in Fig. 1(a). A quasi one-dimensional (1D) BEC is imaged by counting the number of atoms present in subintervals, referred to as pixels in the following, spanning the extent of the system. For simplicity we imagine the probing to occur with unit efficiency, and we note that the recorded data will fluctuate around the quantum-mechanical expectation value of the number of atoms present in each pixel.

A dark soliton is a stationary excited state solution of the Gross-Pitaevskii equation (GPE) [11],

$$0 = \mathcal{H}_{\rm GP}\,\Phi \equiv -\frac{\hbar^2}{2\,m}\frac{\partial^2\Phi}{\partial x^2} + g\,|\Phi|^2\,\Phi - \mu\,\Phi, \qquad (1)$$

where $\Phi(x)$ is the order parameter, m is the atomic mass, g is the effective 1D interaction strength, and μ is the chemical potential. For finite systems Φ is normalized to the number of particles in the gas, and is proportional to the single-particle wave function, self-consistently occupied by all the atoms in a Hartree-Fock product state. When $g > 0$ (repulsive interactions) the dark soliton in

*E-mail: negretti@phys.au.dk

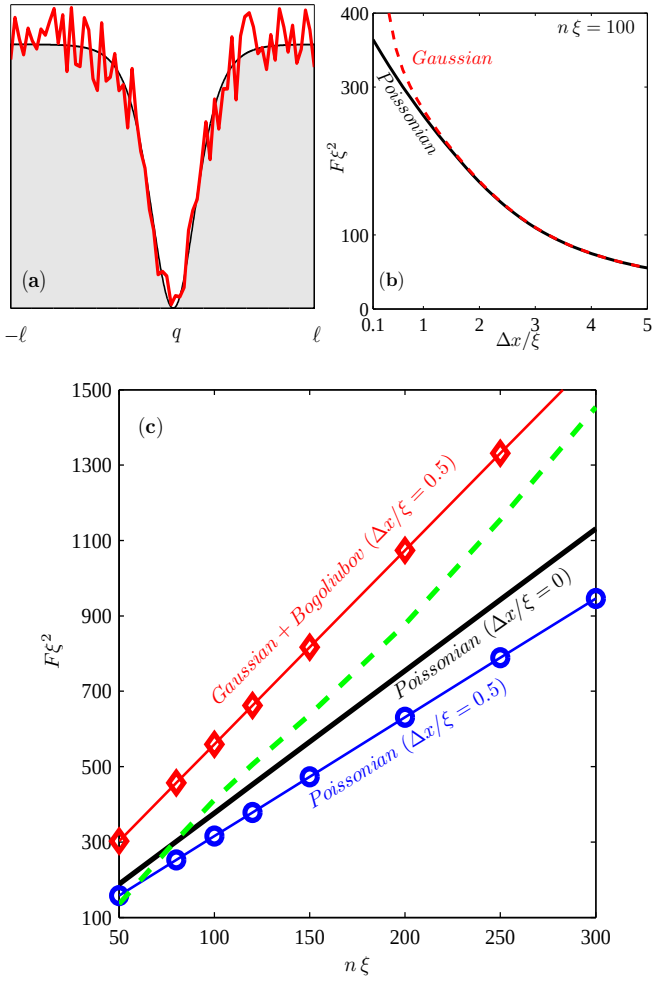

Figure 1: (Color online). (a) Dark soliton density distribution (shaded region) and typical measurement outcome with number fluctuations (red thick curve). (b) Rescaled Fisher information $F\xi^2$ versus pixel size for a mean-field solution with Poisson counting statistics (solid curve) and with a Gaussian continuous approximation (dashed curve). The optimum sensitivity for locating the soliton position is $\Delta q = F^{-1/2}$; $\xi \propto n^{-1/2}$ is the healing length. (c) Rescaled Fisher information versus atomic density: Poissonian distribution (circles), Bogoliubov and Gaussian approximations (diamonds). Continuous thick (black) line represents the behaviour of Eq. (4), whereas the dashed (green) line shows the information extracted from the signal-to-noise ratio for a simple gain function $g(x, n)$ (see text).

the homogeneous case is given by [11]

$$\Phi(x;q) = \sqrt{n}\tanh\left[\kappa(x-q)\right], \qquad (2)$$

where $\kappa = 1/(\sqrt{2}\,\xi)$ is the reciprocal width of the soliton profile, n is the linear density of the condensate, and $\xi = \hbar/\sqrt{2\,m\,g\,n}$ is the healing length. The position of the soliton is described by the parameter q.

When dealing with not truly 1D Bose gases, even in the dimensionality cross-over [12], care has to be taken. Exact 1D solitons are stable because of the integrability of the 1D GPE, while solitons in 3D elongated condensates are thermodynamically unstable because of scattering with thermal excitations [13]. We consider our 1D model to be a good description for the soliton dip uncertainty, especially when a measurement is performed shortly after its preparation [14]. We note also that part of our analysis can be readily generalized to the full 3D description and also to effective 1D descriptions with a suitably modified GPE [15, 16].

The number n_s of atoms in pixel s will on average be equal to the integral of the density $\rho(x;q) = |\Phi(x;q)|^2$ over the pixel area Δx: $\bar{n}_s = \int_{x_s}^{x_s+\Delta x} \mathrm{d}x\,\rho(x;q)$. Due to fluctuations around the quantum-mechanical expectation value, the counting data will be noisy, and we need a theory that provides the best estimator for q. The Cramér-Rao bound provides a lower limit on the minimum uncertainty of a parameter X, determined from measured values of a quantity η, whose conditional probability distribution is given by $p(\eta|X)$. The variance of an unbiased estimator of X is limited from below by $\min[\mathrm{Var}(X)] = 1/F(X)$, where

$$F(X) = -\int \mathrm{d}\eta\, p(\eta|X)\,\frac{\partial^2 \ln p(\eta|X)}{\partial X^2} \qquad (3)$$

is the Fisher information [10]. Let us assume that q is known (by a coarse scale estimate) to within an interval for which a first-order series expansion $\sqrt{\rho(x;q)} \simeq \sqrt{\rho(x;0)} + q\,f(x)$ is precise enough. A mean-field condensate, whether in a total number eigenstate or a coherent state, displays Poissonian counting statistics in each pixel, when registered in a large number of them. An estimator that reaches the CRB is found by weighting the measured data n_s with a weighting function $g(x) \propto f(x)/\rho(x;0)$ [17]. We thus have a procedure by which we can estimate the soliton position optimally.

To identify the CRB we need to evaluate the Fisher information (3), where η is the entire set of (discrete) variables $\{n_s\}$ with a probability distribution that depends on the soliton position q. The Fisher information can be determined analytically, as done in Ref.[17] for a coherent state of light populating a mode with a given spatial density. For our dark soliton (2) we get

$$F = 4\int \mathrm{d}x \left[\frac{\partial\sqrt{\rho(x;q)}}{\partial q}\right]^2 = \frac{16\sqrt{mg}}{3\,\hbar}n^{3/2}. \qquad (4)$$

This dependence on the density is shown in Fig. 1(c) (continuous thick line). The main result is that the smallest value of q that can be distinguished scales as $n^{-3/4}$ with the atomic density. This is a faster convergence with n than the usual shot-noise scaling ($\sim n^{-1/2}$). We emphasize that this enhancement does not require any squeezed or otherwise entangled multiatom state; it follows from a simple (coherent state) macroscopic wave function. Note also that we obtained Eq.(4) by assuming no correlations between different pixels and taking the

limit of infinitely small pixel areas. Fig. 1(b) (thick solid line) shows the dependence of the rescaled Fisher information $F\,\xi^2$ on the pixel size (placing a soliton dip at the border between two pixels).

The dark soliton owes its existence to interactions, but interactions also cause deviations of the exact quantum many-body state from the simple mean-field solution. These deviations cause quantum depletion of the condensate and fluctuations of the soliton dip position, which cannot simply be set to a classical value. We analyze these effects by Bogoliubov theory, and show that, contrary to what may be expected, quantum fluctuations actually increase the optimum sensitivity of the soliton position measurement.

First, we note that the case of Poissonian counting statistics is tractable because the integral (sum) in Eq.(3) over all possible measurement outcomes can be performed analytically. Poisson statistics is fully parametrized by the mean values of the observables, and hence it does not offer the possibility of investigating the role of extra noise or correlations in the gas. We therefore establish a formalism in which it is possible to deviate from Poisson statistics and in which a good approximation to the Fisher information (3) can be computed efficiently. As a natural choice we consider a multi-variate Gaussian approximation for the distribution function of the atomic density, namely

$$p(\mathbf{n}|q) = \frac{(2\,\pi)^{-M_{\rm px}/2}}{\sqrt{\det(\mathbf{C})}}\,\exp\left[-\frac{1}{2}\,(\mathbf{n}-\bar{\mathbf{n}})^{\rm T}\,\mathbf{C}^{-1}\,(\mathbf{n}-\bar{\mathbf{n}})\right]. \quad (5)$$

Here the column vectors $\mathbf{n}$ and $\bar{\mathbf{n}}$ collect the detected stochastic atom number variables and their expectation values, and $M_{\rm px}$ is the total number of pixels. The correlations between atom numbers on the pixels are described by the covariance matrix $\mathbf{C}$.

Inserting (5) in (3) gives the Fisher information as

$$F = \frac{1}{2}\left\{\frac{\partial^2\det(\mathbf{C})/\partial q^2}{\det(\mathbf{C})} - \left[\frac{\partial\det(\mathbf{C})/\partial q}{\det(\mathbf{C})}\right]^2 + \sum_{s,j}\left[\frac{\partial^2(\mathbf{C}^{-1})_{s\,j}}{\partial q^2}\,C_{s\,j} + 2\,(\mathbf{C}^{-1})_{s\,j}\,\frac{\partial\bar{n}_s}{\partial q}\,\frac{\partial\bar{n}_j}{\partial q}\right]\right\}. \quad (6)$$

When Eq.(6) is evaluated for a continuous Gaussian distribution with the same covariance as a discrete Poisson distribution, $C_{s\,j} = {\rm Var}(n_s)\,\delta_{s\,j} = \bar{n}_s\,\delta_{s\,j}$, we get the Fisher information

$$F = \sum_s \frac{1}{\bar{n}_s}\left(\frac{\partial\bar{n}_s}{\partial q}\right)^2 + \frac{1}{2}\sum_s\frac{1}{\bar{n}_s^2}\left(\frac{\partial\bar{n}_s}{\partial q}\right)^2. \quad (7)$$

The first sum is equivalent to the Poisson result, while the second sum is a consequence of our Gaussian approximation. In the limit $\bar{n}_s \gg 1$, where the distributions are similar, this latter term becomes a negligible correction. For infinitely small pixels, however, the Gaussian and Poissonian distributions differ and the second term in Eq.(7) diverges as shown in Fig. 1(b). This divergence is linked to the nonphysical, noninteger, and negative values of n allowed by the Gaussian distribution. In the analysis of real experiments, however, this is not relevant, since detectors will typically not be chosen so small that only one or zero atoms are recorded in some pixels.

III. BOGOLIUBOV–DE GENNES THEORY

In order to determine the quantum fluctuations of the atomic density, we have diagonalized the Bogoliubov–de Gennes operator

$$\mathcal{L}_{\rm BdG} = \begin{pmatrix} \mathcal{H}_{\rm GP} + g\,|\Phi|^2 & g\,\Phi^2 \\ -g\,\Phi^{*2} & -\mathcal{H}_{\rm GP} - g\,|\Phi|^2 \end{pmatrix}. \quad (8)$$

Here, the wave function $\Phi = \Phi(x;q)$ is the stationary mean-field solution given by Eq.(2). Following the approach in Refs.[14, 18], we find that the phonon mode functions $(u_k, v_k) \equiv \left(W_k^+, W_k^-\right)$ of $\mathcal{L}_{\rm BdG}$ in a box with periodic boundary conditions can be written as

$$W_k^\pm(x;q) = \frac{M_k}{\kappa}\,e^{i\,k\,x}\,\left\{k\,{\rm sech}^2[\kappa\,(x-q)] + \beta_k^\pm\,(k/2 + i\,\kappa\,\tanh[\kappa\,(x-q)])\right\}, \quad (9)$$

where M_k is a normalisation constant [19], $\beta_k^\pm = (k/\kappa)^2 \pm 2\,\epsilon_k/(g\,n)$, and $\epsilon_k = \hbar\,c\,|k|\,\sqrt{1+k^2/(4\,\kappa^2)}$.

Before discussing the contribution of the phonon modes, we note that $\mathcal{L}_{\rm BdG}$ in addition has two gapless modes. They are Goldstone modes, originating from the breaking of the translational and the global U(1) phase symmetry if one assumes a definite value of the displacement q, and, e.g., a real order parameter $\Phi(x;q)$. The zero modes together with their adjoint mode functions are [14, 19] (N_0 is the mean atom number in Φ)

$$\begin{aligned} u_q(x;q) &= -i\,\kappa\,\sqrt{n}\,{\rm sech}^2[\kappa\,(x-q)] \\ u_\theta(x;q) &= \Phi(x;q) \\ u_q^{\rm ad}(x;q) &= \frac{-i}{4\,\sqrt{n}} \\ u_\theta^{\rm ad}(x;q) &= \frac{\Phi(x;q) + i\,x\,u_q(x;q)}{2\,(N_0 + n/\kappa)}, \end{aligned} \quad (10)$$

with the associated functions $v_\alpha(x) = -u_\alpha^*(x)$ and $v_\alpha^{\rm ad}(x) = u_\alpha^{{\rm ad}*}(x)$. The quantization box is much larger than ξ, and we neglect small boundary corrections.

We are now in position to compute the mean atomic density and the covariance matrix $\mathbf{C}$ in the Bogoliubov approximation. The total matter-field operator is split into $\hat\Psi(x) = \Phi(x) + \delta\hat\Psi(x)$, with $[\delta\hat\Psi(x), \delta\hat\Psi^\dagger(y)] = \delta(x-y)$, and where $\delta\hat\Psi(x) = \sum_{\alpha=\theta,q}\hat P_\alpha u_\alpha^{\rm ad}(x) - i\,\hat\theta_\alpha u_\alpha(x) + \sum_k \hat b_k u_k(x) + \hat b_k^\dagger v_k^*(x)$ with $[\hat\theta_\alpha, \hat P_\beta] = i\,\delta_{\alpha\beta}$ as in Ref.[14], and $[\hat b_k, \hat b_p^\dagger] = \delta_{kp}$.

The Hamiltonian of the quantized field theory, expanded to second order in $\delta\hat\Psi$ and $\delta\hat\Psi^\dagger$, contains

quadratic terms $\hat{P}_\alpha^2/2m_\alpha$ with effective masses m_α, and the usual phonon number operator contribution. Therefore, in the lowest-energy state (and in thermally excited states) of the system, there are no correlations between the phonon operators and the zero-mode operators.

The average density of atoms is given by

$$\langle\hat{\Psi}^\dagger(x)\hat{\Psi}(x)\rangle = |\Phi(x)|^2 + \sum_k |v_k(x)|^2 + \mathcal{Z}(x), \qquad (11)$$

where

$$\mathcal{Z}(x) = \sum_{\alpha=\theta,q} \Big\{ |u_\alpha^{\rm ad}(x)|^2 \langle\hat{P}_\alpha^2\rangle + |u_\alpha(x)|^2 \langle\hat{\theta}_\alpha^2\rangle - u_\alpha^*(x)\, u_\alpha^{\rm ad}(x) - 2\,\Im[u_\alpha^*(x)\, u_\alpha^{\rm ad}(x)]\, \langle\hat{P}_\alpha\, \hat{\theta}_\alpha\rangle \Big\}, \qquad (12)$$

and the dependence on q has not been displayed explicitly. Given the modes (10), for real Φ, the last term in (12) vanishes, and the zero-mode contribution to the density *at the soliton position* becomes

$$\mathcal{Z}(q) = \frac{n\, q^2\, \kappa^2}{4\,(N_0 + n/\kappa)^2}\, \langle\hat{P}_\theta^2\rangle + \frac{\langle\hat{P}_q^2\rangle}{16\, n} + n\,\kappa^2\, \langle\hat{\theta}_q^2\rangle - \frac{\kappa}{4}. \qquad (13)$$

The operator $\hat{P}_\theta$ reflects the fluctuation in the total condensed atom number. Poisson statistics thus implies $\langle\hat{P}_\theta^2\rangle \simeq N_0$. The soliton position is described by the operator $\hat{\theta}_q$, and behaves like a free particle. We adopt here the strategy, introduced in Ref.[20] for a trapped BEC, choosing the quantum state for the q mode to be the unique Gaussian state in $\hat{P}_q$, $\hat{\theta}_q$ that minimizes the average density $\overline{n}(q) = \langle\hat{\Psi}^\dagger(q)\hat{\Psi}(q)\rangle$. This state has a finite spread $\langle\hat{P}_q^2\rangle$, so it evolves slowly in time, and we consider measurements done quickly, before the spreading of the soliton ultimately invalidates the Bogoliubov approach.

The density correlation function $\mathcal{C}(x,y;q)$ is found by a straightforward expansion of field operator products to second order in $\delta\hat{\Psi}$,

$$\mathcal{C}(x,y;q) = \Phi(x)\Phi(y)\Big\{ \sum_k [u_k(x) + v_k(x)]\, [u_k^*(y) + v_k^*(y)] + 4\left[\langle\hat{P}_\theta^2\rangle u_\theta^{\rm ad}(x) u_\theta^{\rm ad*}(y) + \langle\hat{\theta}_q^2\rangle u_q(x) u_q^*(y)\right]\Big\}. \qquad (14)$$

We finally get the elements of the covariance matrix $\mathbf{C}$ by integrating $\mathcal{C}(x,y;q)$ over finite-size pixels, $x \in [x_j, x_j + \Delta x]$ and $y \in [x_s, x_s + \Delta x]$.

The results of our numerical analysis are presented in Fig.1(c), which shows the Fisher information for both the mean-field and the Bogoliubov descriptions of the condensate, where the latter is computed within the Gaussian approximation. All continuous lines show a linear dependence, which implies in our dimensionless units that the soliton position q can be probed with a sensitivity that scales as $n^{-3/4}$. In Fig.1(c), the dashed line represents the information that can be extracted from the signal-to-noise ratio for a gain function $g(x,n) = \left\{1 - \tanh^2(\kappa x)[1 + \beta(n)]/2\right\} / \tanh(\kappa x)$, where $\beta(n) = \tanh(0.014 n\,\xi - 0.84)$ represents a small correction to the optimal weighting function for a mean-field condensate.

Why does the inclusion of noise in the Bogoliubov description provide an even better resolution than the mean field? To understand this, consider as in Ref.[17] the mean value of the detected signal $\bar{S} \simeq q \int {\rm d}x g(x) \partial_q \rho(x;0)$ (for small q), and its variance $\Delta S^2 = \int {\rm d}x{\rm d}y g(x) g(y) \mathcal{C}(x,y;0)$. The amount of information that can be extracted from this estimation strategy is related to the signal-to-noise ratio $\bar{S}^2/\Delta S^2$. It can be shown from Eq.(14), using the completeness relation for phonon and Goldstone modes, that $\Delta S^2 = \Delta S^2_{\rm MF} + \Delta S^2_{\rm ph} - \Delta S^2_{\rm G}$ for any gain funtion $g(x)$. The Goldstone and phonon contributions, $\Delta S^2_{\rm G}$ and $\Delta S^2_{\rm ph}$, are of the same order in n, but $\Delta S^2_{\rm G}$ dominates and we get smaller noise [19].

IV. CONCLUSIONS

In conclusion, we have used signal processing theory to show that the position of a dark soliton can be measured with a precision that scales more favorably than the usual shot noise. Our study thus illustrates that atomic interactions can enhance the performance of atom interferometers. Scaling below the shot-noise limit is also reported for entangled or squeezed states, but such states are not required in our scheme. Note that a similar potential for high-precision sensors may be achieved with bright solitons [21] and with vortex lattices, or with a "bubble" floating in a BEC and filled with another atomic species [22]. The $n^{-3/4}$ scaling can be understood by simple statistical arguments applied to the mean-field condensate. Our quantitative analysis by means of the Crámer-Rao bound shows, however, that quantum fluctuations due to phonon and Goldstone modes enhance the sensitivity because these modes provide density correlations that are sensitive to the soliton position and make a larger amount of information available.

Acknowledgments

The authors A.N. and K.M. acknowledge financial support from the European Union Integrated Project SCALA, and K.M. acknowledges support from the ONR MURI on quantum metrology with atomic systems. The author C.H. thanks the Deutsche Forschungsgemeinschaft for support (Grant No. He 2849/3). We thank U. V. Poulsen for his comments on the manuscript.

[1] M. R. Andrews, C. G. Townsend, H.-J. Miesner, D. S. Durfee, D. M. Kurn, and W. Ketterle, Science **275**, 637 (1997).

[2] S. Burger, K. Bongs, S. Dettmer, W. Ertmer, K. Sengstock, A. Sanpera, G. V. Shlyapnikov, and M. Lewenstein, Phys. Rev. Lett. **83**, 5198 (1999).

[3] K. W. Madison, F. Chevy, W. Wohlleben, and J. Dalibard, Phys. Rev. Lett. **84**, 806 (2000).

[4] Z. Dutton, M. Budde, C. Slowe, and L. V. Hau, Science **293**, 663 (2001).

[5] G.-B. Jo, J.-H. Choi, C. A. Christensen, T. A. Pasquini, Y.-R. Lee, W. Ketterle, and D. E. Pritchard, Phys. Rev. Lett. **98**, 180401 (2007).

[6] A. Negretti, and C. Henkel, J. Phys. B: At. Mol. Opt. Phys. **37**, L385 (2004).

[7] V. Giovannetti, S. Lloyd, and L. Maccone, Science **306**, 1330 (2004).

[8] P. Bouyer, and M. A. Kasevich, Phys. Rev. A **56**, R1083 (1997).

[9] L. Pezzè, and A. Smerzi, Europhys. Lett. **78**, 30004 (2007).

[10] P. Réfrégier, in *Noise Theory and Application to Physics*, (Springer, New York, 2004).

[11] L. P. Pitaevskii, and S. Stringari, in *Bose-Einstein Condensation*, International Series of Monographs on Physics No. 116 (Oxford University, New York, 2003).

[12] G. Theocharis, P. G. Kevrekidis, M. K. Oberthaler, and D. J. Frantzeskakis, Phys. Rev. A **76**, 045601 (2007).

[13] A. Muryshev, G. V. Shlyapnikov, W. Ertmer, K. Sengstock, and M. Lewenstein, Phys. Rev. Lett. **89**, 110401 (2002).

[14] J. Dziarmaga, Phys. Rev. A **70**, 063616 (2004).

[15] L. Salasnich, A. Parola, and L. Reatto, Phys. Rev. A **65**, 043614 (2002).

[16] A. M. Mateo and V. Delgado, Phys. Re. A **77**, 013617 (2008).

[17] V. Delaubert, N. Treps, C. Fabre, H. A. Bachor, and P. Réfrégier, Europhys. Lett. **81**, 44001 (2008).

[18] Th. Busch, in *Theoretical Studies of Degenerate Inhomogeneous Atomic Gases*, Ph.D. thesis, University of Innsbruck (2000).

[19] A. Negretti, C. Henkel, and K. Mølmer, In preparation.

[20] J. Dziarmaga, and K. Sacha, Phys. Rev. A **66**, 043620 (2002)

[21] T. Vaughan, P. Drummond, and G. Leuchs, Phys. Rev. A **75**, 033617 (2007).

[22] S. G. Bhongale, and E. Timmermans, e-print arXiv:0711.4007.